

Saturation Power based Simple Energy Efficiency Maximization Schemes for MU-MISO Systems

Jaehoon Jung, Sang-Rim Lee, and Inkyu Lee, *Senior Member, IEEE*

School of Electrical Eng., Korea University, Seoul, Korea

Email: {jhnjung, sangrim78, inkyu}@korea.ac.kr

Abstract

In this paper, we investigate an energy efficiency (EE) maximization problem in multi-user multiple input single output downlink channels. The optimization problem in this system model is difficult to solve in general, since it is in non-convex fractional form. Hence, conventional algorithms have addressed the problem in an iterative manner for each channel realization, which leads to high computational complexity. To tackle this complexity issue, we propose a new simple method by utilizing the fact that the EE maximization is identical to the spectral efficiency (SE) maximization for the region of the power below a certain transmit power referred to as *saturation power*. In order to calculate the saturation power, we first introduce upper and lower bounds of the EE performance by adopting a maximal ratio transmission beamforming strategy. Then, we propose an efficient way to compute the saturation power for the EE maximization problem. Once we determine the saturation power corresponding to the maximum EE in advance, we can solve the EE maximization problem with SE maximization schemes with low complexity. The derived saturation power is parameterized by employing random matrix theory, which relies only on the second order channel statistics. Hence, this approach requires much lower computational complexity compared to a conventional scheme which exploits instantaneous channel state information, and provides insight on the saturation power. Numerical results validate that the proposed algorithm achieves near optimal EE performance with significantly reduced complexity.

I. INTRODUCTION

The material in this paper was presented in part at the IEEE International Conference on Communications (ICC), London, UK, June 2015 [1].

Exponentially increasing service demands for wireless communications have mainly required much higher transmission rate, which leads to increased energy consumption [2], [3]. Recently, the energy consumption has been regarded as a crucial parameter when designing wireless networks, since low energy efficient transmission has a negative impact on the environment and hamper sustainable development. Thus, from the perspective of green communications, energy efficiency (EE) has received a lot of attentions for future wireless communication systems [4]. The EE is defined as the ratio of the sum rate to the total power consumption measured in bit/Joule.

Many researches have addressed EE solutions for various system model scenarios [5]–[13]. In [14], the EE problem was formulated by exploiting dirty paper coding and the uplink-downlink duality in broadcasting channels. While this work presented a performance upper bound for broadcasting channels, many practical constraints exist due to high complexity. For general scenarios with inter-user interference (IUI), the optimization problem for EE remains non-convex, and thus it is difficult and more challenging to solve. Recently, EE schemes based on linear beamforming were studied for multiple-input single-output (MISO) interfering broadcasting channels [10]. By transforming the fractional programming into linear programming [5] and applying the weighted minimum mean square error (WMMSE) approach in [15], a local optimal solution was obtained in [10]. However, this algorithm solved the EE problem in an iterative manner for each channel realization that gives rise to high computational complexity. Moreover, it is difficult to get insight on the system performance without resorting to Monte Carlo simulations.

To tackle these issues mentioned above, we investigate a simple and practical EE maximization scheme in multi-user (MU) MISO downlink channels. First, we observe that the EE value obtained from the EE maximization problem is saturated at a certain transmit power, which will be referred to as *saturation power*. Then, the problem of the EE maximization becomes identical to that of the spectral efficiency (SE) maximization for the region below. As a result, the EE maximization problem can simply be computed from the SE maximization by identifying the saturation power.

However, the optimum saturation power for the EE maximization scheme in considered system models is difficult to compute. Hence, we first attempt to derive lower and upper bounds of the EE performance by applying maximal ratio transmission (MRT) beamforming. Then, the saturation power of the lower and upper bounds of the EE are presented in closed form by employing random matrix theory [16]–[19]. Here, based on the relationship of the derived

saturation power and the EE performance, we can efficiently determine the saturation power by exploiting an interpolation method. It is noted that the optimal saturation power is bounded by the derived saturation power for the lower and upper bounds of the EE. Consequently, utilizing the derived saturation power, we can solve the EE problem efficiently by only adopting the SE maximization scheme. Numerical results validate that the proposed algorithm achieves near optimal EE performance with much lower complexity.

The rest of the paper is comprised as follows: Section II presents a system model and the problem formulation. In Section III, the relationship between EE and SE is described briefly. Then, we derive the saturation power based on large system analysis and suggest a simplified scheme for the EE maximization utilizing the derived saturation power in Section IV. From the simulation results in Section V, we confirm the validity of the proposed method. Finally, this paper is terminated with conclusions in Section VI.

Throughout the paper, we adopt lowercase and uppercase boldface letters for vectors and matrices, respectively. The superscript $(\cdot)^H$ stands for conjugate transpose. In addition, $\|\cdot\|$ and $\text{tr}(\cdot)$ represent Euclidean 2-norm and trace, respectively. Also, \mathbf{I}_d denotes an identity matrix of size d . A set of N dimensional complex column vectors is expressed by \mathbb{C}^N .

II. SYSTEM MODEL

In this paper, we consider an MU-MISO channel with bandwidth W where a base station (BS) equipped with M transmit antennas serves N users with a single antenna. Then, the received signal y_k at the k -th user ($k = 1, \dots, N$) is given by

$$y_k = \sqrt{p_k} \mathbf{h}_k^H \mathbf{v}_k s_k + \sum_{j \neq k} \sqrt{p_j} \mathbf{h}_k^H \mathbf{v}_j s_j + n_k$$

where p_k is the transmit power consumed by the k -th user satisfying $\sum_{k=1}^N p_k \leq P$ [Watt/Hz] in order to satisfy BS transmit power constraint PW , $\mathbf{h}_k \in \mathbb{C}^M$ defines the flat fading channel vector from the BS to the k -th user with the coherence time T , \mathbf{v}_k means the beamforming vector for the k -th user with $\|\mathbf{v}_k\|^2 = 1$, $s_k \sim \mathcal{CN}(0, 1)$ represents the complex data symbol intended for the k -th user, and $n_k \sim \mathcal{CN}(0, \sigma^2)$ stands for the additive white Gaussian noise at the k -th user.

For notational conveniences, we denote $\{\mathbf{p}\}$ and $\{\mathbf{v}\}$ as a set of all transmit power values and

beamforming vectors, respectively. Then, the individual rate of the k -th user is computed as

$$R_k(\{\mathbf{p}\}, \{\mathbf{v}\}) = \log(1 + \text{SINR}_k(\{\mathbf{p}\}, \{\mathbf{v}\}))$$

where $\text{SINR}_k(\{\mathbf{p}\}, \{\mathbf{v}\})$ indicates the individual signal-to-interference-plus-noise-ratio (SINR) for the k -th user as

$$\text{SINR}_k(\{\mathbf{p}\}, \{\mathbf{v}\}) = \frac{|\mathbf{h}_k^H \mathbf{v}_k|^2 p_k}{\sum_{j \neq k} |\mathbf{h}_k^H \mathbf{v}_j|^2 p_j + \mathcal{N}_0}.$$

Here, \mathcal{N}_0 represents $\mathcal{N}_0 = \sigma^2/W$. During a time-frequency block TW , the total amount of the transmitted information is given by

$$TW \sum_k \log_2(1 + \text{SINR}_k). \quad [\text{bits}]$$

From an EE point of view, we consider the power consumption for a BS [10], [20], where the total power consumption during the time-frequency block TW is modeled as

$$P_T(\{\mathbf{p}\}) = TW \left(\xi \sum_k p_k \|\mathbf{v}_k\|^2 + P_{const} \right). \quad [\text{Joule}] \quad (1)$$

Here, $\xi \geq 1$ stands for an inefficiency of the power amplifier and P_{const} equals $P_{const} = MP_c + P_o$ where P_c is defined as $P_c = \frac{P'_c}{W}$ with P'_c being the constant circuit power consumption proportional to the number of radio frequency chains, and P_o means $P_o = \frac{P'_o}{W}$ with P'_o indicating the static power at the BS which is independent of the number of transmit antennas.

Then, the EE is defined as the ratio of the sum rate to the total power consumption

$$\text{EE}(\{\mathbf{p}\}, \{\mathbf{v}\}) = \frac{\sum_k R_k(\{\mathbf{p}\}, \{\mathbf{v}\})}{P_T(\{\mathbf{p}\})}.$$

Therefore, the EE maximization problem can be formulated by

$$\begin{aligned} & \max_{\{\mathbf{p}\}, \{\mathbf{v}\}} \quad \text{EE}(\{\mathbf{p}\}, \{\mathbf{v}\}) \\ & \text{s.t.} \quad \sum_{k=1}^N p_k \leq P. \end{aligned} \quad (2)$$

It is noted that problem (2) is non-convex because of coupled interference and the fractional form, and thus computing a solution of the problem is quite complicated. In [10], a local optimal

solution of the EE for interfering broadcasting channels was obtained by two layer optimization adopting a linear subtractive form. However, it should be solved in an iterative manner for each channel realization, which gives rise to high computational complexity. In what follows, we focus on a simple algorithm which can solve the EE maximization with reduced complexity.

III. PROPERTIES OF ENERGY EFFICIENCY

In this section, we investigate the characteristics of the EE. Based on the properties of the EE described in this section, the derivation of the saturation power is triggered to optimize the EE performance in a simple manner. It is interesting to note that the EE performance is saturated once the total transmit power exceeds a certain point, which we call saturation power. Then, the maximization of the EE becomes identical to that of the SE for the region below the saturation power. To explain this, we consider a simple EE model for the transmit power P as

$$\text{EE}(P) = \frac{R(P)}{P + P_{static}} \quad (3)$$

where $R(P) = \log(1 + P)$ and P_{static} indicates the static power consumption term.

From this EE expression (3), the optimal transmit power P_{EE} which maximizes the EE can be calculated in closed form as [5]

$$P_{EE} = \exp\left(\mathcal{W}_0\left(\frac{P_{static} - 1}{e}\right) + 1\right) - 1$$

where $\mathcal{W}_0(\cdot)$ denotes the principal branch of the Lambert W function defined as the inverse function of $f(x) = xe^x$.

For the transmit power region below P_{EE} , full transmit power should be applied to achieve the maximal performance of the EE. This is due to the fact that when the total transmit power is fully consumed at the region below the saturation power, the consumed power becomes constant which does not affect the EE optimization. In this case, the considered problem is equivalent to the sum rate maximization. This suggests that transmitting the maximum available power is most energy efficient at this region. In the same way, the SE performance can be maximized at the same region because the rate $R(P)$ is monotonically increasing function with respect to P . In contrast, for the region above the saturation power, consuming full power at the BS degrades the EE performance, since a sum rate gain cannot compensate for the increased power consumption in the EE.

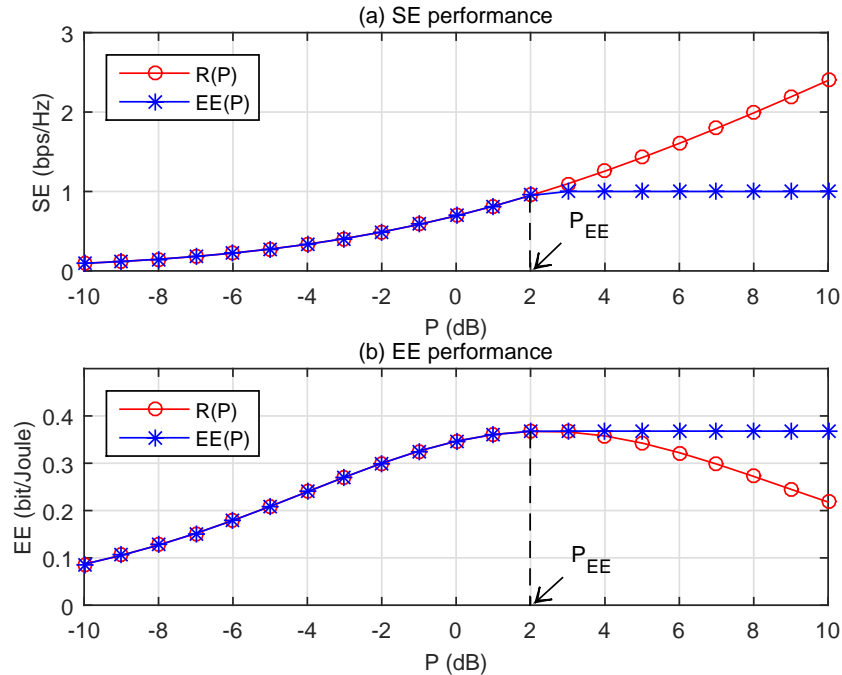


Fig. 1. Comparison of SE and EE for equation (3) in terms of the transmit power P (a) SE performance and (b) EE performance

In Figure 1, we illustrate the performance curves of the SE and EE for equation (3) with respect to the transmit power P . In this example, the saturation power P_{EE} is shown to be about 2 dB. It can be observed that the SE maximization is identical to the EE maximization when the transmit power P is smaller than the saturation power P_{EE} . Also, P_{EE} corresponds to the power which yields the maximal SE. In Figure 1 (a), the EE scheme achieves the same rate as the SE scheme for $P \leq P_{EE}$, while the rate of the EE scheme becomes saturated for $P \geq P_{EE}$, since the EE scheme fixes the power at P_{EE} to maximize the EE. Meanwhile, the SE algorithm always transmits at full power for maximizing the SE even after the saturation power P_{EE} . In Figure 1 (b), the SE scheme exhibits a performance loss in terms of the EE because a gain of the rate cannot make up for the impact of the increased power consumption as mentioned before.

IV. DERIVATION OF SATURATION POWER

In this section, motivated by properties of the EE shown in Section III, we first focus on determining the saturation power which starts to yield the saturated EE performance. Unfortu-

nately, the EE solution in [10] requires iterative methods, and thus it is not possible to obtain the saturation power in closed form. Alternatively, we address lower and upper bounds of the EE performance to allow simple computations of the saturation power. From the derived lower and upper bounds of the EE, we can identify the saturation power corresponding to each bound of the EE in a closed form solution. Then, by utilizing the determined saturation power, we propose a new EE maximization scheme only adopting the SE maximization method with reduced complexity. For mathematical tractability, we assume that the transmit power of each user p_k for $k = 1, \dots, N$ is equally allocated.

A. Saturation Power for a Lower Bound of EE

First, we start with obtaining a lower bound of the EE performance. One simple precoding which can serve as a lower bound is MRT beamforming which employs $\mathbf{v}_{k,MRT} = \frac{\mathbf{h}_k}{\|\mathbf{h}_k\|}$. In this case, the EE for MRT η_{MRT} with equal power allocation can be expressed as

$$\eta_{MRT} = \frac{\sum_{k=1}^N \log(1 + \text{SINR}_{k,MRT})}{\xi P + P_{const}} \quad (4)$$

where $\text{SINR}_{k,MRT}$ is given by

$$\text{SINR}_{k,MRT} = \frac{|\mathbf{h}_k^H \mathbf{v}_{k,MRT}|^2 \frac{P}{N}}{\sum_{j \neq k} |\mathbf{h}_k^H \mathbf{v}_{j,MRT}|^2 \frac{P}{N} + \mathcal{N}_0}. \quad (5)$$

It is clear that $\text{SINR}_{k,MRT}$ changes for every channel realizations. To avoid calculating these instantaneous channel gains, we apply random matrix theory in (5). It is worth noting that in the asymptotic regime, the channel gain values become deterministic which depends only on the second order channel statistics and the randomness according to instantaneous channel realizations disappears. Although the parameters are obtained in the large system limit, we will show in the simulation section that this approximation is well matched even for small dimensions.

To derive large system results, we will utilize the lemma in [21] which assumes that the number of users N and the number of transmit antennas M grow large with $\frac{N}{M}$ at a fixed ratio. We emphasize that the asymptotic analysis is used only to derive deterministic channel gain values, and the system which we consider in this paper has a finite dimension. From [21], we can calculate the deterministic value for both the desired signal power $|\mathbf{h}_k^H \mathbf{v}_{k,MRT}|^2$ and the interference signal power $|\mathbf{h}_k^H \mathbf{v}_{j,MRT}|^2$ in (5). First, the desired signal power for MRT is written

by

$$|\mathbf{h}_k^H \mathbf{v}_{k,MRT}|^2 = \frac{|\mathbf{h}_k^H \mathbf{I}_M \mathbf{h}_k|^2}{\|\mathbf{h}_k\|^2} = \mathbf{h}_k^H \mathbf{I}_M \mathbf{h}_k.$$

Then, using the trace lemma in [22], we have

$$\mathbf{h}_k^H \mathbf{I}_M \mathbf{h}_k - \text{tr}(\mathbf{I}_M) \xrightarrow{a.s.} 0. \quad (6)$$

Also, the interference signal power for MRT is determined in a similar manner as

$$|\mathbf{h}_k^H \mathbf{v}_{j,MRT}|^2 = \frac{|\mathbf{h}_k^H \mathbf{I}_M \mathbf{h}_j|^2}{\|\mathbf{h}_j\|^2} = \frac{\mathbf{h}_k^H \mathbf{I}_M \mathbf{h}_j \mathbf{h}_j^H \mathbf{I}_M \mathbf{h}_k}{\mathbf{h}_j^H \mathbf{h}_j}. \quad (7)$$

After some mathematical manipulations, the numerator and denominator terms for the interference signal power in (7) converge almost surely as

$$\begin{aligned} \mathbf{h}_k^H \mathbf{I}_M \mathbf{h}_j \mathbf{h}_j^H \mathbf{I}_M \mathbf{h}_k &- \text{tr}(\mathbf{I}_M^2) \xrightarrow{a.s.} 0, \\ \mathbf{h}_j^H \mathbf{h}_j &- \text{tr}(\mathbf{I}_M) \xrightarrow{a.s.} 0. \end{aligned}$$

Then, the interference signal power $|\mathbf{h}_k^H \mathbf{v}_{j,MRT}|^2$ is given by

$$\frac{\mathbf{h}_k^H \mathbf{I}_M \mathbf{h}_j \mathbf{h}_j^H \mathbf{I}_M \mathbf{h}_k}{\mathbf{h}_j^H \mathbf{h}_j} - 1 \xrightarrow{a.s.} 0. \quad (8)$$

By replacing the deterministic channel gain values in (6) and (8) into $\text{SINR}_{k,MRT}$, the asymptotic EE for MRT η_{MRT}° is presented as

$$\eta_{MRT}^\circ = \frac{\sum_{k=1}^N \log(1 + \text{SINR}_{k,MRT}^\circ)}{\xi P + P_{const}} \quad (9)$$

where $\text{SINR}_{k,MRT}^\circ$ is denoted as

$$\text{SINR}_{k,MRT}^\circ = \frac{MP}{(N-1)P + NN_0}.$$

We can note that $\text{SINR}_{k,MRT}^\circ$ is a function of P and is no longer dependent on channel realizations. As a result, η_{MRT}° can be identified only based on given system configurations. To obtain the saturation power for a lower bound of the EE, we utilize equation (9) for the following theorem.

Theorem 1: A lower bound of η_{MRT}° , defined by η_{LB} , is expressed by

$$\eta_{LB} = \frac{NMP}{(\xi P + P_{const})\{(N + M - 1)P + N\mathcal{N}_0\}}.$$

Then, the saturation power P_{LB} corresponding to the EE lower bound η_{LB} is computed by

$$P_{LB} = \sqrt{\frac{N\mathcal{N}_0 P_{const}}{\xi(N + M - 1)}}. \quad (10)$$

Proof: The numerator term of (9) is reformulated by

$$\begin{aligned} N \log \left(1 + \frac{MP}{(N - 1)P + N\mathcal{N}_0} \right) &= N \log \frac{(N + M - 1)P + N\mathcal{N}_0}{(N - 1)P + N\mathcal{N}_0} \\ &= -N \log \left(1 - \frac{MP}{(N + M - 1)P + N\mathcal{N}_0} \right). \end{aligned} \quad (11)$$

From the fact that the term $\frac{MP}{(N + M - 1)P + N\mathcal{N}_0}$ is smaller than 1, equation (11) can be bounded by adopting the relationship $\log(1 + x) \leq x$ for $|x| < 1$ as

$$-N \log \left(1 - \frac{MP}{(N + M - 1)P + N\mathcal{N}_0} \right) \geq \frac{NMP}{(N + M - 1)P + N\mathcal{N}_0} \triangleq R_{LB}. \quad (12)$$

Consequently, the lower bounded EE η_{LB} is presented by

$$\eta_{LB} = \frac{R_{LB}}{\xi P + P_{const}}. \quad (13)$$

Then, the saturation power P_{LB} can be determined by differentiating η_{LB} in (13) with respect to P . Thus, P_{LB} which maximizes η_{LB} is calculated from the following equation as

$$(N + M - 1)\xi P_{LB}^2 = N\mathcal{N}_0 P_{const}.$$

From this equation, we arrive at (10) ■

According to the result in Theorem 1, the saturation power for a lower bound of EE is obtained with a closed form expression (10).

B. Saturation Power for an Upper Bound of EE

In the previous subsection, a lower bound for the EE is found by applying MRT with equal power allocation. Now, we derive an upper bound of the EE by ignoring the effect of IUI. Then,

the EE with no IUI, η_{no-IUI} , can be given by

$$\eta_{no-IUI} = \frac{\sum_{k=1}^N \log \left(1 + \frac{|\mathbf{h}_k^H \mathbf{v}_{k,MRT}|^2 P}{N_0 N} \right)}{\xi P + P_{const}}. \quad (14)$$

When the IUI is not considered, the numerator term of η_{no-IUI} is maximized by the MRT beamforming because the beam is aligned with the channel for the intended user. Therefore, the EE performance is upper bounded by η_{no-IUI} .

By employing the large system analysis as in Section IV-A, the numerator of η_{no-IUI} in (14) is presented as

$$\log \left(1 + \frac{|\mathbf{h}_k^H \mathbf{v}_{k,MRT}|^2 P}{N_0 N} \right) - R_{UB} \xrightarrow{a.s.} 0 \quad (15)$$

where R_{UB} is defined as $R_{UB} \triangleq N \log \left(1 + \frac{M}{N N_0} P \right)$. Then, an asymptotic upper bound of the EE, denoted by η_{UB} , is expressed as

$$\eta_{UB} = \frac{R_{UB}}{\xi P + P_{const}}. \quad (16)$$

To compute the saturation power for the EE upper bound η_{UB} , we address the following theorem.

Theorem 2: The saturation power P_{UB} which maximizes η_{UB} is written by

$$P_{UB} = \frac{N N_0}{M} \left[\exp \left(1 + \mathcal{W}_0 \left(\frac{1}{e} \left(\frac{M P_{const}}{N N_0 \xi} - 1 \right) \right) \right) - 1 \right]. \quad (17)$$

Proof: By differentiating η_{UB} with respect to the total transmit power P , it follows

$$\frac{d\eta_{UB}}{dP} = \frac{N}{(\xi P + P_{const})^2} \left[\frac{M}{N N_0} \frac{\xi P + P_{const}}{1 + \frac{M}{N N_0} P} - \xi \log \left(1 + \frac{M}{N N_0} P \right) \right]. \quad (18)$$

For the saturation power P_{UB} corresponding to η_{UB} , setting equation (18) to zero yields

$$\frac{M}{N N_0} (\xi P_{UB} + P_{const}) - \xi s \log s = 0$$

where $s = 1 + \frac{M}{N N_0} P_{UB}$.

Then, we have

$$\frac{M P_{const}}{N N_0 \xi} - 1 = s(\log s - 1).$$

With the Lambert W function, this form can be solved by a closed form expression as

$$\log s = 1 + \mathcal{W}_0 \left(\frac{1}{e} \left(\frac{MP_{const}}{N\mathcal{N}_0\xi} - 1 \right) \right).$$

Since $\mathcal{W} \left(\frac{1}{e} \left(\frac{MP_{const}}{N\mathcal{N}_0\xi} - 1 \right) \right) \geq -1$, which is guaranteed by $s \geq 1$ for $P_{UB} \geq 0$, the principal branch of the Lambert W function \mathcal{W}_0 is selected. From this equation, we can reach the saturation power P_{UB} in (17). ■

C. Relationship among P_{LB} , P_{UB} , and the optimal saturation power P^*

From the previous subsections, the saturation power for lower and upper bounds of the EE has been derived. In this subsection, we address the property of the optimal saturation power denoted as P^* related to P_{LB} and P_{UB} . As already mentioned, the average sum rate of the SE maximization scheme denoted by R_{SE} is clearly bounded between R_{LB} in (12) and R_{UB} in (15). From this, we will show that the optimal saturation power P^* lies between P_{LB} and P_{UB} by adopting the linear parametric programming approach.

It can be seen that the optimization problem (2) belongs to fractional programming. Hence, this problem can be transformed into parametric programming as in [5]. We consider the following equivalent form of the fractional program in (2) as

$$\begin{aligned} & \max_{\{\mathbf{p}\}, \{\mathbf{v}\}, \lambda \in \mathbb{R}} \quad \lambda \\ & \text{s.t.} \quad \sum_k R_k(\{\mathbf{p}\}, \{\mathbf{v}\}) - \lambda P_T(\{\mathbf{p}\}) \geq 0. \end{aligned}$$

For a given parameter λ , it is noted that the optimization problem is referred to as a feasibility problem in $\{\mathbf{p}\}$ and $\{\mathbf{v}\}$. Therefore, the optimal value of the parameter λ can be found by using a bisection method for the feasibility problem at each step of the algorithm [23].

Defining a function $F(\lambda)$ as

$$F(\lambda) = \max_{\{\mathbf{p}\}, \{\mathbf{v}\}} \sum_k R_k(\{\mathbf{p}\}, \{\mathbf{v}\}) - \lambda P_T(\{\mathbf{p}\}),$$

it is obvious that $F(\lambda)$ is convex and strictly decreasing in λ . Moreover, this is regarded as bi-criterion optimization such that $\sum_k R_k(\{\mathbf{p}\}, \{\mathbf{v}\})$ is maximized while $P_T(\{\mathbf{p}\})$ is minimized. The parameter λ determines the relative weight of the total power consumption $P_T(\{\mathbf{p}\})$.

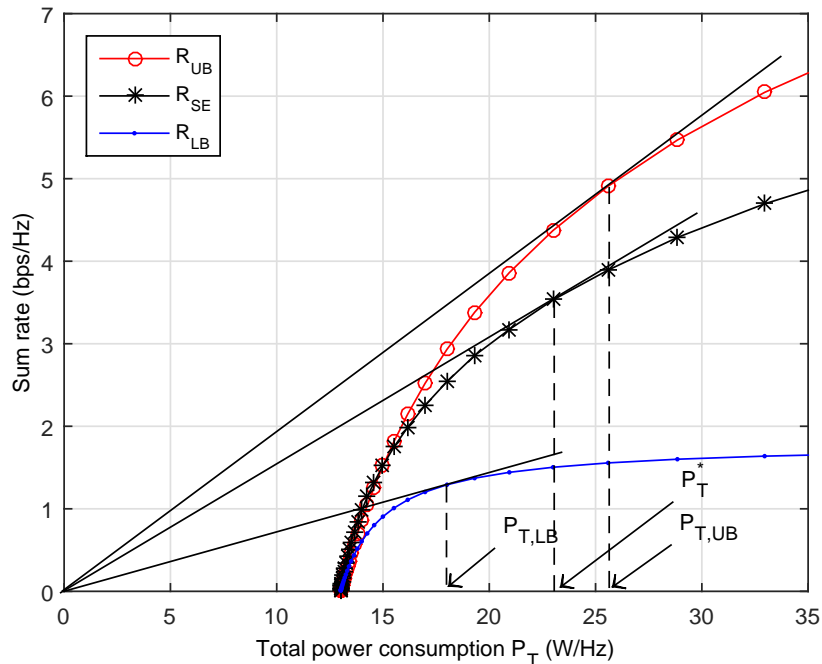


Fig. 2. Trade-off curves between sum rate and total consumed power with $P'_c = 30$ dBm and $P'_o = 40$ dBm

For this bi-criterion problem, the set of Pareto-optimal values is called the optimal trade-off curve [5]. As presented in [10], solving problem (2) is equivalent to finding the root of the nonlinear function $F(\lambda)$, i.e., $F(\lambda) = 0$. In other words, λ means the slope of the tangent for the trade-off curve and the optimal λ denoted by λ^* occurs when $F(\lambda^*) = 0$. Then, by exploiting these properties of the linear parametric programming, we can address the relationship among P_{LB} , P_{UB} , and P^* .

From the trade-off curves in Figure 2, we can identify the slope of the tangent for R_{LB} , R_{SE} , and R_{UB} . In this figure, the trade-off curve is illustrated between the sum rate and the total power consumption in (1) with $N = M = 3$ and $P_{const} = 13$. We can see that the SE performance R_{SE} is certainly bounded as $R_{LB} < R_{SE} < R_{UB}$ for all P_T . Here, $P_{T,LB}$, P_T^* , and $P_{T,UB}$ denote the total power consumption at the BS for R_{LB} , R_{SE} , and R_{UB} , respectively. It is noted that the optimal power consumption for each scheme is defined as a contact point with each sum rate curve and the corresponding tangent.

Then, the saturation power is calculated by subtracting P_{const} from the optimal power consumption, e.g., $P_{LB} = P_{T,LB} - P_{const}$. As shown in the figure, the saturation power for each

scheme has the relationship of $P_{LB} < P^* < P_{UB}$. Accordingly, the achieved EE values which equal the slope of the tangent for each sum rate are given as $\eta_{LB}(P_{LB}) < \eta_{SE}(P^*) < \eta_{UB}(P_{UB})$ where $\eta_{SE}(P^*) = \frac{R_{SE}(P^*)}{\zeta P^* + P_{const}}$ represents the maximum EE value for η_{SE} corresponding to the saturation power P^* . Therefore, utilizing this property, we quantify the optimal saturation power P^* as a function of P_{LB} and P_{UB} in the following.

D. Proposed EE Scheme based on the Saturation Power

From the derived saturation power for lower and upper bounds of the EE, we will determine the saturation power P^* . To this end, we adopt an interpolation method in a similar way to [24]. First, the maximum value of η_{SE} is defined by $\gamma_{SE} = \eta_{SE}(P^*)$. Also, the maximum EE value for the lower and upper bounds γ_{LB} and γ_{UB} are denoted by $\eta_{LB}(P_{LB})$ and $\eta_{UB}(P_{UB})$, respectively. Then, the proposed saturation power P_{prop} can be computed as a point between P_{LB} and P_{UB} by exploiting the relationship between the saturation power and the corresponding EE value for each bound. For instance, if γ_{SE} is close to γ_{UB} , the saturation power P^* should be set near P_{UB} .

Therefore, we consider the following relation on the difference between various bounds addressed in Section IV-C as

$$\frac{\gamma_{UB} - \gamma_{SE}}{\gamma_{UB} - \gamma_{LB}} : \frac{\gamma_{SE} - \gamma_{LB}}{\gamma_{UB} - \gamma_{LB}} = \frac{P_{UB} - P_{prop}}{P_{UB} - P_{LB}} : \frac{P_{prop} - P_{LB}}{P_{UB} - P_{LB}}. \quad (19)$$

After some mathematical manipulations, equation (19) is expressed as

$$P_{UB} - P_{prop} = G(P_{prop} - P_{LB}),$$

where the EE gap G represents

$$G = \frac{\gamma_{UB} - \gamma_{SE}}{\gamma_{SE} - \gamma_{LB}}. \quad (20)$$

Then, the proposed saturation power P_{prop} can be calculated as

$$P_{prop} = \omega P_{LB} + (1 - \omega) P_{UB} \quad (21)$$

where $\omega = \frac{G}{1+G}$ means the weight factor between P_{LB} and P_{UB} .

In fact, it is not possible to obtain G directly since γ_{SE} is unknown. Therefore, in order to

compute the EE gap G , we consider regularized zero forcing (RZF) beamforming [21]. The relation between γ_{SE} and the maximum EE performance for RZF γ_{RZF} can be formulated by $\gamma_{SE} = \beta\gamma_{RZF}$, where a constant $\beta > 1$ accounts for the performance gain of η_{SE} over η_{RZF} . In what follows, we determine γ_{RZF} which will be used in calculating G in (20) for a given β .

By adopting random matrix theory in [21], the asymptotic EE performance for RZF η_{RZF}° is expressed as

$$\eta_{RZF}^\circ = \frac{\sum_{k=1}^N \log(1 + \text{SINR}_{k,RZF}^\circ)}{\xi \sum_{k=1}^N p_k + P_{const}}$$

where $\text{SINR}_{k,RZF}^\circ$ is obtained as

$$\text{SINR}_{k,RZF}^\circ = \frac{(m_k^\circ)^2}{\Gamma_k^\circ + \frac{\Psi^\circ}{\rho}(1 + m_k^\circ)^2}.$$

Here, the deterministic equivalent values m_k° , Γ_k° , and Ψ° are derived in [21] for RZF and $\rho = P/\mathcal{N}_0$. These parameters are affected by p_k for $\forall k$.

Assuming equal power allocation with uncorrelated channels, the deterministic equivalent for all users has the same value, i.e., $m_k^\circ = m^\circ$ and $\Gamma_k^\circ = \Gamma^\circ$. Then, the η_{RZF}° with equal power allocation denoted by η_{RZF} can be calculated as

$$\eta_{RZF} = \frac{N \log \left(1 + \frac{(m^\circ)^2 P}{\Gamma^\circ P + \Psi^\circ (1 + m^\circ)^2 \mathcal{N}_0} \right)}{\xi P + P_{const}}.$$

To determine the maximum EE for RZF γ_{RZF} , η_{RZF} is differentiated with respect to P and is set to zero as

$$\frac{d\eta_{RZF}}{dP} = \frac{N(m^\circ)^2 A}{\{((m^\circ)^2 + \Gamma^\circ)P + A\}(\Gamma^\circ P + A)(\xi P + P_{const})} - N \log \left(1 + \frac{(m^\circ)^2 P}{\Gamma^\circ P + A} \right) \frac{\xi}{(\xi P + P_{const})^2} = 0 \quad (22)$$

where $A = \Psi^\circ(1 + m^\circ)^2 \mathcal{N}_0$. Here, we define the function $f(P)$ to identify the saturation power P_{RZF} for η_{RZF} as

$$f(P) = \log \left(1 + \frac{(m^\circ)^2 P}{\Gamma^\circ P + A} \right) - \frac{(m^\circ)^2 A (P + \frac{P_{const}}{\xi})}{\{((m^\circ)^2 + \Gamma^\circ)P + A\}(\Gamma^\circ P + A)}.$$

It is interesting to note that the function $f(P)$ is monotonically increasing with respect to P and the equation $f(P) = 0$ has a unique solution. Also, $f(P)$ converges to $-\frac{(m^\circ)^2 P_{const}}{\zeta A}$ for $P \rightarrow 0$ and $\log(1 + (m^\circ)^2/\Gamma^\circ)$ for $P \rightarrow \infty$. Therefore, the EE saturation power P_{RZF} can be

computed simply by one dimensional search and the maximum EE performance can be obtained as $\gamma_{RZF} = \eta_{RZF}(P_{RZF})$. Consequently, after γ_{SE} is replaced by $\beta\gamma_{RZF}$, we can determine the saturation power P_{prop} in (21).

Now, we propose a simplified EE maximization scheme by utilizing the derived saturation power P_{prop} . In the simplified scheme, a solution of the SE maximization problem is adopted for the original EE maximization problem. First, when the available transmit power P is less than P_{prop} , the SE maximization scheme is conducted with full power P to maximize the EE performance. On the contrary, if P is greater than P_{prop} , the fixed transmit power P_{prop} is used with the SE maximization method. In summary, after the saturation power P_{prop} is calculated in (21), the SE maximization algorithm in [15] is processed with the transmit power given by $\min(P_{prop}, P)$ to generate a beamforming solution.

Next, we briefly address the computational complexity. The structure of the EE algorithm in [10] is comprised by the outer layer and the inner layer optimization. The outer layer searches for the EE parameter η , while the inner layer solves the non-fractional subtractive problem for a given η computed at the outer layer. Thus, the inner layer algorithm should be executed whenever the EE parameter is updated at the outer layer, and this causes high computational complexity.

The complexity of the algorithm in [15] is similar to that of the inner layer part in [10]. It is noted that the SE maximization algorithm in [15] is processed only once in the proposed EE scheme. Moreover, when determining the saturation power P_{prop} , we have P_{LB} and P_{UB} in closed form which depends only on the second order channel statistics and the estimation of γ_{SE} needs simple one-dimensional search. Hence, the complexity of our proposed algorithm is much lower than that of the EE algorithm in [10]. The computation time of the algorithm in [10] is contingent on the convergence threshold δ for the outer layer and it takes about ten times higher than that of the proposed scheme with $\delta = 10^{-3}$, while the EE performance of the proposed scheme is quite close to that of the algorithm in [10].

V. NUMERICAL RESULTS

In this section, we verify the validity of our proposed method through Monte Carlo simulations. The numbers of users N and transmit antennas M are equal to 3 unless specified otherwise. Also, we adopt the bandwidth $W = 20$ MHz, the noise spectral density $\mathcal{N}_0 = -174$ dBm/Hz, noise figure $N_F = 7$ dB and the inefficiency of the power amplifier $\xi = 1$. The circuit power

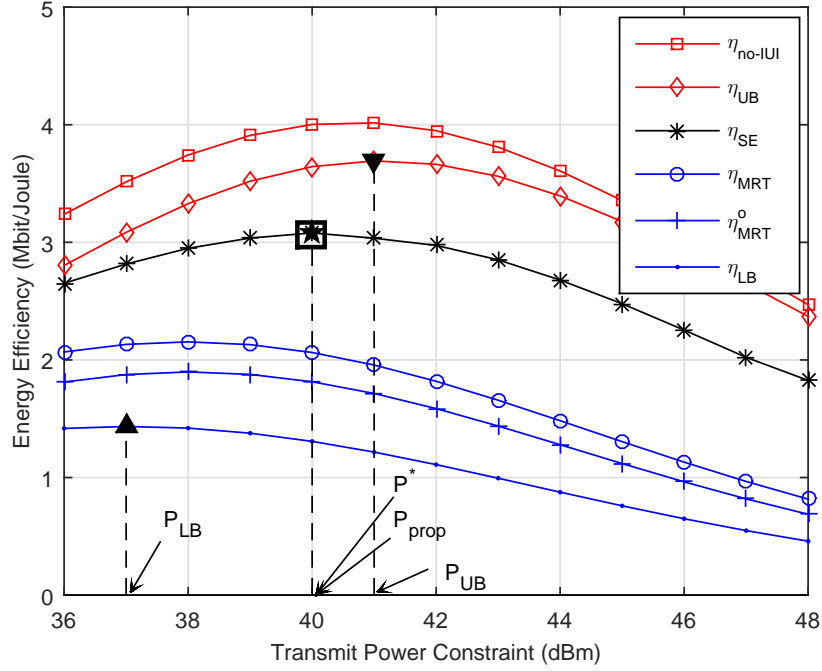


Fig. 3. Comparison of the saturation power with $P'_c = 30$ dBm and $P'_o = 40$ dBm

per antenna P'_c and the static power consumed at the BS P'_o are set to 30 dBm and 40 dBm, respectively.

First, we evaluate the saturation power derived in Section IV in Figure 3. Here, regular and inverted triangles mean the maximum EE for (10) and (17), respectively, and P_{LB} and P_{UB} are computed as the derived saturation power corresponding to these maximum points shown in (10) and (17). Also, star and rectangular marks denote the EE performance of the SE maximization scheme η_{SE} obtained by the saturation power P^* and P_{prop} , respectively. It is noted that the saturation power for the lower and upper bounds of the EE is the same as the values calculated by (10) and (17), respectively. Moreover, P_{prop} is quite well matched with the true saturation power P^* . This demonstrates that our approach of determining the saturation power generates an accurate estimate of the actual saturation power. When computing P_{prop} , we find that $\beta = 1.3$ achieves the maximum EE performance through numerical simulations. Note that the optimal β may change when system parameters vary. Nevertheless, it can be observed that the proposed saturation power P_{prop} using the fixed β yields performance nearly identical to that of P^* for various conditions.

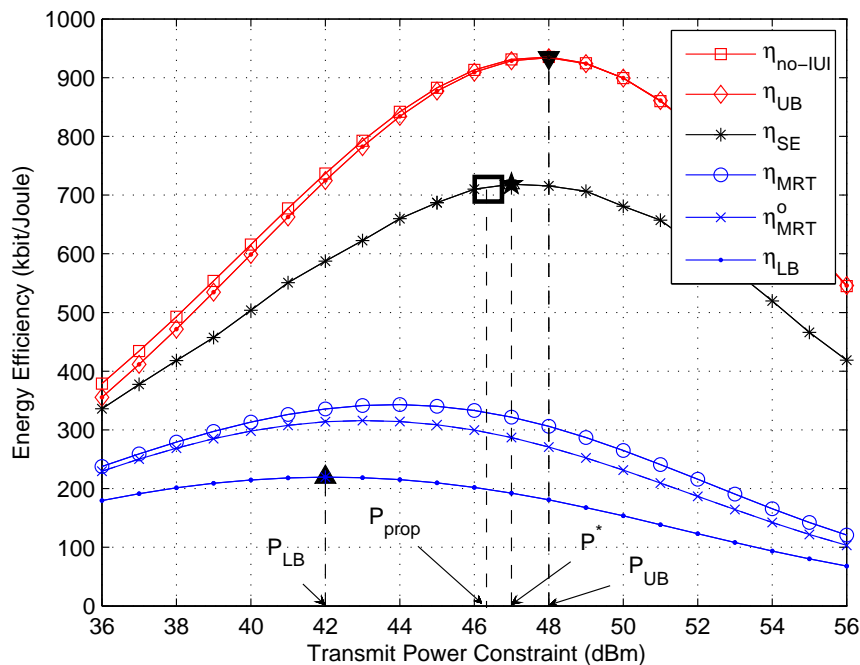


Fig. 4. Comparison of the saturation power with $P'_c = 40$ dBm and $P'_o = 50$ dBm

Figure 4 exhibits the comparison of the saturation power for $P'_c = 40$ dBm and $P'_o = 50$ dBm. Again in this figure, the saturation power derived by (10) and (17) match well with high accuracy. In this case, P^* is slightly larger than P_{prop} . Despite the gap between the saturation power, the EE performance corresponding to P_{prop} is very close to the maximum EE in [10]. Moreover, the average EE performance η_{UB} and η_{MRT}^o obtained from the large system analysis are quite close to that of η_{no-IUI} and η_{MRT} for the finite system case, respectively. Therefore, we can conclude that even for a system with finite dimension, the analysis of the EE performance with the large system limit provides an accurate approximation.

Next, we validate the EE performance of the proposed scheme based on the derived saturation power in Figure 5 with $N = M$. In this figure, it is observed that the EE performance becomes larger when M and N are increased from 2 to 4. Note that compared to the EE maximization algorithm in [10], almost the same EE performance is achieved by the proposed method with P_{prop} which utilizes the SE maximization scheme with much reduced complexity. Also, in Figure 6, we demonstrate the EE performance for $P'_c = 40$ dBm and $P'_o = 50$ dBm. It is remarkable that the proposed scheme with P_{prop} produces the EE performance quite close to the optimal

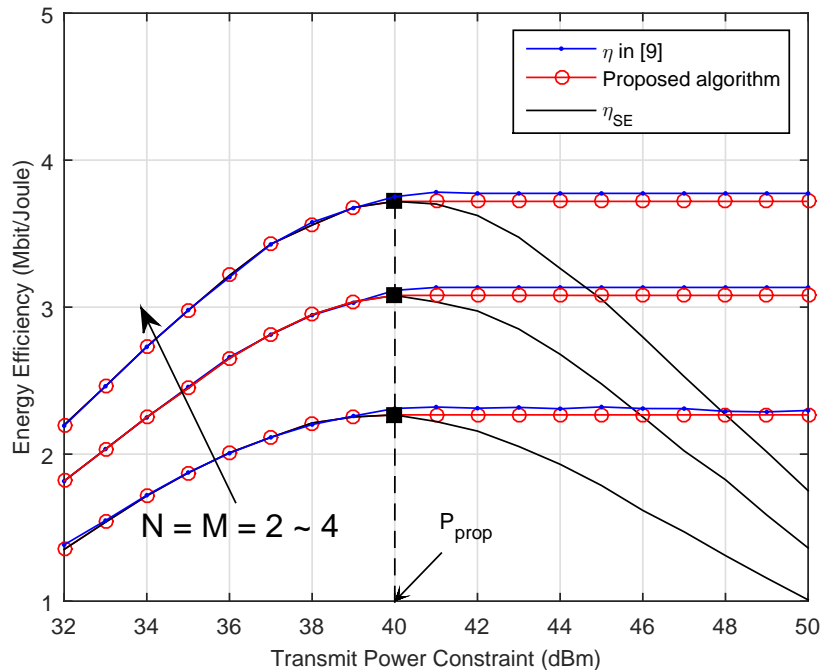


Fig. 5. EE performance of the proposed algorithm with $P'_c = 30$ dBm and $P'_o = 40$ dBm

EE solution in [10] for different configurations. Furthermore, the derived saturation power gives insight for the BS power designs in terms of the EE.

Finally, we exhibit the effect of the EE performance with respect to the constant power consumption term P_{const} . Comparing Figures 5 and 6, when P_{const} increases, the saturation power for achieving the maximum EE also becomes large while the performance of the EE is decreased. In Figure 7, this phenomenon is illustrated by the trade-off curve of the sum rate and the total consumption power. In the plot, the curves with circular and rectangular marks denote the sum rate for the SE maximization scheme with $P_{const} = 5$ and 15, respectively. We can see that for a larger P_{const} , the trade-off curve is shifted to the right. Then, the optimal slope of the tangent which accounts for the performance of the EE becomes small. On the contrary, the required saturation power is increased to achieve the optimal slope of the tangent. From these results, we confirm that reducing the amount of P_{const} has a main impact on improving the performance of the EE and saving the transmit power consumption.

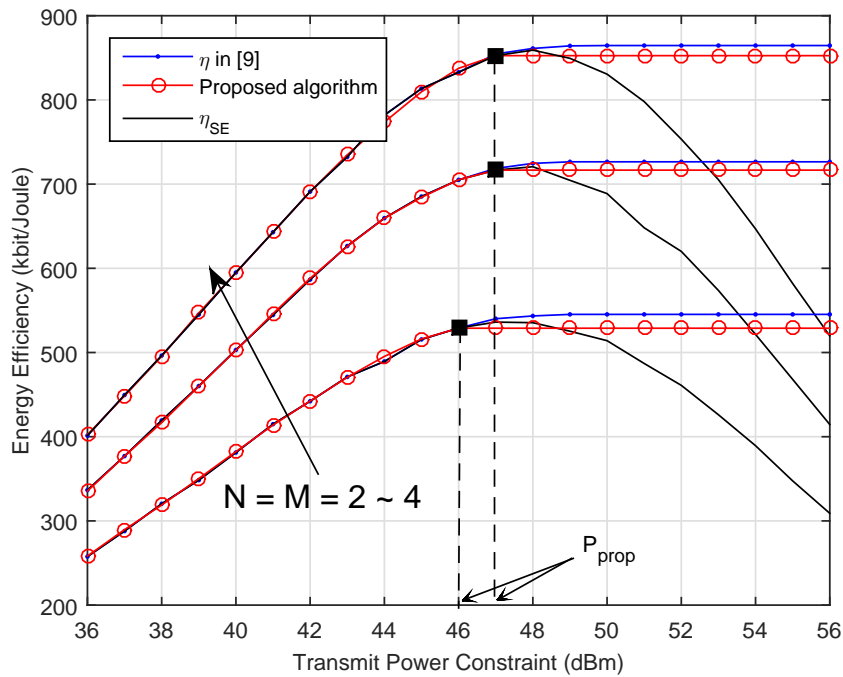


Fig. 6. EE performance of the proposed algorithm with $P'_c = 40$ dBm and $P'_o = 50$ dBm

VI. CONCLUSIONS

In this paper, we have proposed a simple scheme to solve the EE maximization problem for MU-MISO channels. Leveraging the relationship between EE and SE, the EE is maximized by only utilizing the SE maximization scheme based on the saturation power. From large system analysis, we have determined the saturation power corresponding to the maximal EE in closed form by exploiting the property between lower and upper bounds of the EE. This asymptotic result provides insight into the saturation power of the EE for various system configurations. As a result, the proposed EE scheme makes it possible to provide solutions for the EE maximization efficiently. It is noted that a performance loss of the proposed scheme is quite small compared to the optimal EE maximization scheme in [10], and the computational complexity of the proposed scheme is significantly reduced. Also, the simulations demonstrate that the asymptotic results are well matched even for the finite system case.

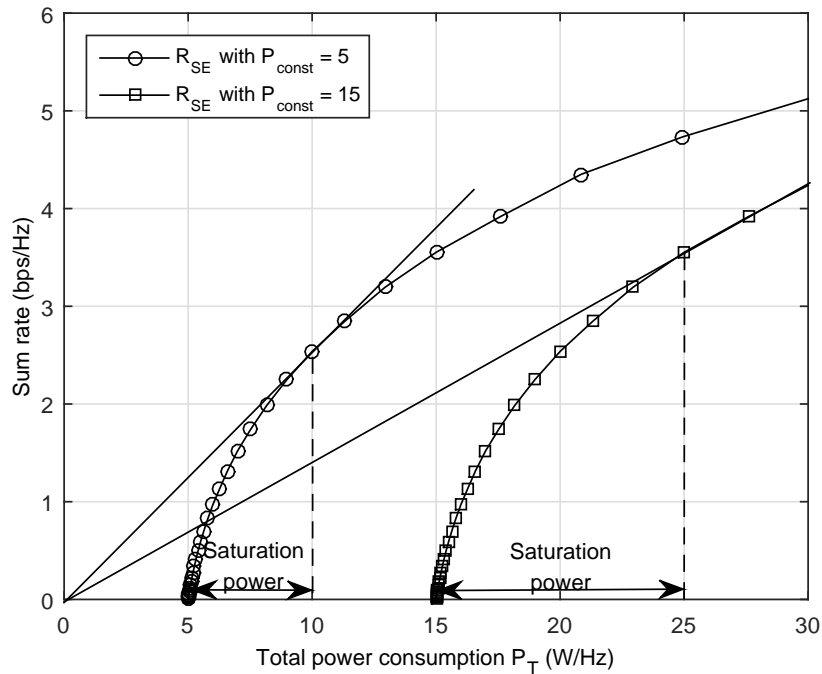


Fig. 7. The impact of the EE performance and the saturation power with respect to constant power consumption P_{const}

REFERENCES

- [1] J. Jung, S.-R. Lee, and I. Lee, "Simple energy efficiency maximization methods for MU-MISO systems based on saturation power," in *Proc. IEEE ICC '15*, pp. 2381 – 2386, June 2015.
- [2] S.-H. Park, H. Park, H. Sung, and I. Lee, "Regularized Transceiver Designs for Multi-User MIMO Interference Channels," *IEEE Transactions on Communications*, vol. 60, pp. 2571–2579, September 2012.
- [3] H. Park, S.-H. Park, J.-S. Kim, and I. Lee, "SINR Balancing Techniques in Coordinated Multi-Cell Downlink Systems," *IEEE Transactions on Wireless Communications*, vol. 12, pp. 626–635, February 2013.
- [4] Y. Chen, S. Zhang, S. Xu, and G. Y. Li, "Fundamental Trade-offs on Green Wireless Networks," *IEEE Communications Magazine*, vol. 49, pp. 30–37, June 2011.
- [5] C. Isheden, Z. Chong, E. Jorswieck, and G. Fettweis, "Framework for Link-Level Energy Efficiency Optimization with Informed Transmitter," *IEEE Transactions on Wireless Communications*, vol. 11, pp. 2946–2957, August 2012.
- [6] D. W. K. Ng, E. S. Lo, and R. Schober, "Energy-Efficient Resource Allocation in OFDMA Systems with Large Numbers of Base Station Antennas," *IEEE Transactions on Wireless Communications*, vol. 11, pp. 3292–3304, September 2012.
- [7] D. W. K. Ng, E. S. Lo, and R. Schober, "Energy-Efficient Resource Allocation in Multi-Cell OFDMA Systems with Limited Backhaul Capacity," *IEEE Transactions on Wireless Communications*, vol. 11, pp. 3618–3631, October 2012.
- [8] F. Hélot, M. A. Imran, and R. Tafazolli, "Energy-Efficiency based Resource Allocation for the Orthogonal Multi-user Channel," in *Proc. IEEE VTC '12*, pp. 1–5, September 2012.
- [9] H. Kim, E. Park, H. Park, and I. Lee, "Beamforming and Power Allocation Designs for Energy Efficiency Maximization in MISO Distributed Antenna Systems," *IEEE Communications Letters*, vol. 17, pp. 2100–2103, November 2013.

- [10] S. He, Y. Huang, S. Jin, and L. Yang, "Coordinated Beamforming for Energy Efficient Transmission in Multicell Multiuser Systems," *IEEE Transactions on Communications*, vol. 61, pp. 4961–4971, December 2013.
- [11] E. Björnson, M. Kountouris, and M. Debbah, "Massive MIMO and small cells: Improving energy efficiency by optimal soft-cell coordination," in *Proc. 20th International Conference on Telecommunications*, May 2013.
- [12] H. Q. Ngo, E. G. Larsson, and T. L. Marzetta, "Energy and Spectral Efficiency of very Large Multiuser MIMO Systems," *IEEE Transactions on Communications*, vol. 61, pp. 1436–1449, April 2013.
- [13] S.-R. Lee, H.-B. Kong, H. Park, and I. Lee, "Beamforming Designs Based on an Asymptotic Approach in MISO Interference Channels," *IEEE Transactions on Wireless Communications*, vol. 12, pp. 6430–6438, December 2013.
- [14] J. Xu and L. Qiu, "Energy Efficiency Optimization for MIMO Broadcast Channels," *IEEE Transactions on Wireless Communications*, vol. 12, pp. 690–701, February 2013.
- [15] Q. Shi, M. Razaviyayn, Z.-Q. Luo, and C. He, "An Iteratively Weighted MMSE Approach to Distributed Sum-Utility Maximization for a MIMO Interfering Broadcast Channel," *IEEE Transactions on Signal Processing*, vol. 59, pp. 4331–4340, September 2011.
- [16] R. Couillet, S. Wagner, and M. Debbah, "Asymptotic Analysis of Correlated Multi-Antenna Broadcast Channels," in *Proc. IEEE WCNC*, April 2009.
- [17] H. Huh, S.-H. Moon, Y.-T. Kim, I. Lee, and G. Caire, "Multi-Cell MIMO Downlink with Cell Cooperation and Fair Scheduling: A Large-System Limit Analysis," *IEEE Transactions on Information Theory*, vol. 57, pp. 7771–7786, December 2011.
- [18] J. Hoydis, S. ten Brink, and M. Debbah, "Massive MIMO in the UL/DL of Cellular Networks: How many antennas do we need?," *IEEE Journal on Selected Areas in Communications*, vol. 31, pp. 160–171, February 2013.
- [19] R. Zakhour and S. V. Hanly, "Min-Max Power Allocation in Cellular Networks with Coordinated Beamforming," *IEEE Journal on Selected Areas in Communications*, vol. 31, pp. 287–302, February 2013.
- [20] E. Björnson, L. S. J. Hoydis, and M. Debbah, "Optimal Design of Energy-Efficient Multi-User MIMO Systems: Is Massive MIMO the Answer?," *IEEE Transactions on Wireless Communications*, vol. 14, pp. 3059–3075, June 2015.
- [21] S. Wagner, R. Couillet, M. Debbah, and D. T. M. Slock, "Large System Analysis of Linear Precoding in Correlated MISO Broadcast Channels Under Limited Feedback," *IEEE Transactions on Information Theory*, vol. 58, pp. 4509–4537, July 2012.
- [22] R. Couillet and M. Debbah, *Random Matrix Methods for Wireless Communications*. 1st ed. Cambridge University Press, 2011.
- [23] S. Boyd and L. Vandenberghe, *Convex Optimization*. Cambridge University Press, 2004.
- [24] J. Kim, K.-J. Lee, C. K. Sung, and I. Lee, "A Simple SNR Representation Method for AMC Schemes of MIMO systems with ML Detector," *IEEE Transactions on Communications*, vol. 57, pp. 2971–2976, October 2009.